

Stabilities of Highly Conjugated Radicals from Bond Homolysis Rates

David A. Robaugh[†] and Stephen E. Stein*

Contribution from the National Bureau of Standards, Chemical Kinetics Division, Gaithersburg, Maryland 20899. Received April 5, 1985

Abstract: Rates of Benzyl C-CH₃ homolysis of 4-ethylstyrene (2), 1-phenyl-1-butene (3), 1,1'-diphenylethane (4), 2,2'-diphenylpropane (5), and 1-methylindene (6) were measured in a very low pressure pyrolysis apparatus. Observed rate constants were fit by the following high-pressure Arrhenius expressions with use of RRKM theory

$$k_2/s^{-1} = 10^{15.3} \exp(-35930/T) \quad 1096-1186 \text{ K}$$

$$k_3/s^{-1} = 10^{15.3} \exp(-33970/T) \quad 1030-1115 \text{ K}$$

$$k_4/s^{-1} = 10^{15.5} \exp(-34020/T) \quad 1000-1066 \text{ K}$$

$$k_5/s^{-1} = 10^{15.7} \exp(-33060/T) \quad 950-1054 \text{ K}$$

$$k_6/s^{-1} = 10^{16.0} \exp(-35230/T) \quad 1031-1168 \text{ K}$$

where *A* factors were estimated by comparison to *A* factors for analogous reactions of alkylbenzenes. Differences between activation energies for reactions 2-6 and corresponding alkylbenzene homolysis reactions were used to find "extra" resonance stabilization energies (kcal mol⁻¹) for the following radicals: H₂C=CH-Ph-CH₂·, 1.6; Ph-CH=CH-CH₂·, 5.4; (Ph)₂CH·, 4.5; (Ph)₂CCH₃·, 4.0; and In·, 1.2 (4.184 J = 1 cal). These results are in agreement with predictions of Structure Resonance Theory. In addition, product mass spectra were not consistent with the results of recent shock tube studies of ethylbenzene decomposition where benzyl C-H homolysis was reported to be faster than benzyl C-C homolysis.

Free radicals in which the odd electron is delocalized over a conjugated π -electron network are significantly more stable than comparable nondelocalized radicals. A practical measure of the net stability resulting from delocalization is the difference between bond dissociation enthalpies (BDE) for molecules which lead to stabilized radicals (*R_s*·) and comparable nondelocalized radicals (*R_{ns}*·). This difference in BDE has been called resonance stabilization energy (RSE):

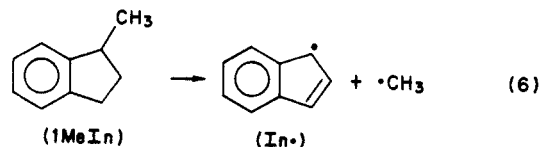
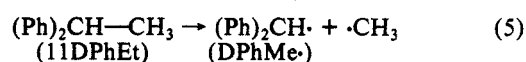
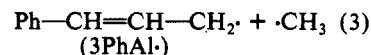
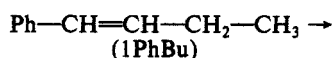
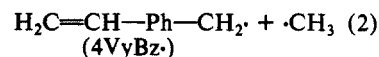
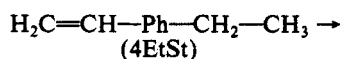
$$RSE(R_s\cdot) \equiv BDE(R_{ns} - X) - BDE(R_s - X) \quad (1)$$

To illustrate, the benzyl C-H bond in toluene is ~10 kcal mol⁻¹ (4.184 J = 1 cal) weaker than primary C-H bonds in alkanes. The RSE for the benzyl radical is therefore equal to 10 kcal mol⁻¹.

Both the ease of formation and reactivity of stabilized radicals are directly dependent on their RSEs; therefore, it is essential to have a reliable means of predicting RSEs in order to accurately analyze the kinetics of reactions involving these radicals. The need for RSE predictive methods is most acute in the analysis of reactions of aromatic compounds, where one must often choose between a large number of pathways involving different aromatic radicals.

A recent review by McMillen and Golden¹ shows that RSEs have been measured for relatively few radicals. Current predictive methods for π -electron energies are useful for estimating RSEs, but these are semiempirical and in need of testing and parametrization with a broader base of experimental data.² Moreover, strain energy and steric inhibition of resonance are not easily obtained from these theories, although they may play a role in determining RSEs; there is almost no quantitative data in this area on which to base estimation methods.

To add to the data base for stabilized radicals, we have used the very low pressure pyrolysis (VLPP) technique to measure rates for the following homolysis reactions:



There have been no previous determinations of rate constants for these reactions nor reports of RSEs for the above radicals. In this study we analyze rate data by comparing them to our previously determined rate data for benzyl C-CH₃ homolysis in structurally related alkylbenzenes. The activation energy obtained for each reaction 2-6 is compared to the activation energy for the corresponding alkylbenzene homolysis reaction and differences related to "extra" amounts of RSE(ΔRSE) in the benzylic radical products of reactions 2-6. This type of comparative VLPP study, by examining pyrolyses under identical experimental conditions, minimizes systematic errors and permits a relatively direct and reliable determination of differences in radical stabilities. Experimental values of ΔRSE are compared to predictions of

(1) McMillen, D. F.; Golden, D. M. *Annu. Rev. Phys. Chem.* **1982**, *33*, 493.

(2) (a) Herndon, W. C. *J. Org. Chem.* **1981**, *46*, 2119. (b) Stein, S. E.; Golden, D. M. *J. Org. Chem.* **1977**, *42*, 839.

[†] Present address, Midwest Research Institute, 425 Volker Boulevard, Kansas City, MO 64110.

Table I. Reactor Parameters

reactor	vol (mL)	aperture area (mm ²)	collision no.	collision freq ω (s ⁻¹)	escape rate ^a constant k_e (s ⁻¹)
3 mm	75.0	9.1	1160	$5.1 \times 10^3 (T/M)^{1/2}$	$4.0 \times (T/M)^{1/2}$

^a Includes a 0.91 Clausing factor.⁵

Structure-Resonance Theory (SRT),² a semiempirical method capable of estimating RSEs. SRT is used here because of its ease of application and the fact that it has already been partly verified by Golden et al.³ for several polycyclic aryl methyl radicals.

Experimental Section

Principles and practice of VLPP have been reviewed previously.⁴ The apparatus used here has been described elsewhere.⁵ Reactor parameters are presented in Table I. Reagents were obtained from the Chemical Samples Co.⁶ and each was thoroughly degassed until a constant vapor pressure was obtained.

Results and Discussion

Product Analysis. Decomposition products were monitored with a quadrupole mass spectrometer and identified by their parent molecular ions by using the lowest possible ionization energies (11–16 eV) to minimize fragmentation. In view of questions raised recently concerning the initial dissociation step in the thermolysis of alkylbenzenes,⁷ product studies are reported here in detail.

Products from the pyrolysis of 4-ethylstyrene (4EtSt) produced three major mass spectral peaks: *m/e* 117, 15, and 118. Peaks at *m/e* 117 and 15 were assumed to correspond to 4-vinylbenzyl radical (4VyBz \cdot) and methyl radical, respectively, products of reaction 2. On the basis of past experience in VLPP experiments,^{4,5} a small fraction of 4VyBz \cdot was expected to abstract H atoms at the walls of the reactor,⁸ hence the signal at *m/e* 118, which was about 24% of the intensity of *m/e* 117 at the highest reaction temperatures, was assumed to correspond to 4-methylstyrene. Two minor peaks at *m/e* 116 (C₉H₈⁺) and 104 (C₈H₈⁺) were observed at ca. 10% of the intensities of *m/e* 117. Because relative intensities of all product signals were independent of flow rate and *m/e* 15 was the only low mass product found, we assumed *m/e* 116 and 104 to correspond to secondary decomposition products or cracking peaks of 4VyBz \cdot .

Products from 1-phenyl-1-butene (1PhBu) produced two major peaks, *m/e* 116 and 15. The peak at *m/e* 15 was assumed to correspond to methyl radicals; however, there was no detectable signal at *m/e* 117 corresponding to 3-phenylallyl radicals (3PhAl \cdot), the other expected product of reaction 3. Instead, *m/e* 116 was found as the major product peak. Typically in VLPP experiments radical products are often found to decompose to more stable products because of the high reactor temperatures involved.⁴ Because relative intensities of *m/e* 116 and 15 were found to be independent of flow rate, we assumed *m/e* 116 to correspond to a secondary decomposition product of 3PhAl \cdot . We suspect that this product was either indene, resulting from an intramolecular radical addition (ring closure) in 3PhAl \cdot followed by loss of an H atom, or phenylallene, formed by a direct loss of H atom from 3PhAl \cdot . No attempt was made to establish the exact identity of this product.

Product spectra of 1,1-diphenylethane (11DPhEt) included the following: *m/e* 167, 166, and 15. As before, we assumed *m/e* 167 and 15 corresponded to the primary decomposition products of reaction 4, namely diphenylmethyl radical (DPhMe \cdot) and

methyl radical, respectively. Signals at *m/e* 166 were generally 30% of intensities of *m/e* 167, but at the highest reaction temperatures (>80% substrate decomposition) this signal grew to about the same intensity as *m/e* 167. Relative intensities of *m/e* 167 to 166 were also found to be independent of flow rate. Here again we assumed *m/e* 166 to correspond to a decomposition product of DPhMe \cdot . The most likely identity of this product is fluorene formed by intramolecular radical addition in DPhMe \cdot followed by loss of an H atom. One minor peak at *m/e* 168 was also observed. We attribute this peak to H-atom abstraction by DPhMe \cdot at the walls to form diphenylmethane.

Pyrolysis of 2,2-diphenylpropane (22DPhPr) produced two major product peaks: *m/e* 180 and 15. The peak at *m/e* 15 was again attributed to methyl radical. There was no detectable signal at *m/e* 181 corresponding to 1,1-diphenylethyl radicals (DPhEt \cdot), the radical product of benzyl C–CH₃ homolysis in 22DPhPr. It is very common in VLPP studies for radicals with weakly bonded β -hydrogens to rapidly decompose to olefins.⁴ One possibility, therefore, is that the peak at *m/e* 180 corresponds to 1,1'-diphenylethene formed by loss of an H atom from DPhEt \cdot . Alternately, this peak may be due to 9-methylfluorene formed by ring closure in DPhEt \cdot followed by a loss of an H atom, the same reaction discussed earlier for DPhMe \cdot . Again, no attempt was made to identify this product. Relative intensities of all product peaks were independent of flow rate.

Products from 1-methylindene (1MeIn) produced peaks at *m/e* 115 and 15 which we attributed to the decomposition products of reaction 6, indenyl radical (In \cdot) and methyl radical, respectively. Only one minor signal at *m/e* 116 was observed at ~6% of the intensity of *m/e* 115. We assumed this peak to correspond to indene.

Product mass spectra indicate that all pyrolyses proceed almost entirely (>96%) by way of benzyl C–CH₃ homolysis. Similarly, in previous studies of ethylbenzene, isopropylbenzene, and *tert*-butylbenzene, which were performed in the same reactor and under the same experimental conditions used here,⁵ product analyses also indicated benzyl C–CH₃ bond rupture. In these earlier studies, mass spectra (14–16 eV) contained peaks at *m/e* 15, which we assigned to methyl radical, as the major low mass product. All higher *m/e* peaks could be attributed to the benzylic radical products formed from C–CH₃ homolysis. No evidence in any product study for direct CH₄ elimination could be found. Also there were no discernible signals one or two mass units less than those of the reactant's parent ions; thus the rate of benzyl C–H homolysis or direct elimination of H₂ could be no greater than 4% of the rate of benzyl C–CH₃ homolysis.

Product analyses in these and previous studies are not consistent with the results of recent shock tube studies by Troe and co-workers⁷ of ethylbenzene decomposition (1250–1600 K). They reported benzyl C–H homolysis as the first dissociation step based on the spectroscopic (UV) observation of the formation of 1-phenyl-1-ethyl radical and styrene in real time. They also reported that benzyl C–CH₃ homolysis was not a major pathway. The reasons for the discrepancy between our work and that of Troe and co-workers are unclear, and studies in our laboratory are now underway to resolve this question. For now we wish to point out the following. In our previous product study of ethylbenzene, peaks at *m/e* 91 and 15, corresponding to benzyl and methyl radicals, were the only major signals observed in mass spectra. In addition, in our isopropylbenzene study,⁵ styrene was found as the major product. This indicated benzyl C–CH₃ homolysis in the substrate leading to the 1-phenyl-1-ethyl radical, which subsequently loses an H atom to form styrene. These are the same products that would be expected if benzyl C–H homolysis occurred in ethylbenzene. Therefore, if 1-phenyl-1-ethyl radicals were formed in our ethylbenzene experiments, we would have detected a peak at *m/e* 104. This evidence along with the combined results of all of our present product studies clearly indicated that benzyl C–CH₃ homolysis is the major decomposition pathway for all molecules discussed here.

VLPP Rate Data. In each study, percentage reaction was determined by monitoring the disappearance of the reactant's

(3) McMillen, D. F.; Trevor, P. L.; Golden, D. M. *J. Am. Chem. Soc.* **1980**, *102*, 7400.

(4) Golden, D. M.; Spokes, G. N.; Benson, S. W. *Angew. Chem., Int. Ed. Engl.* **1973**, *12*, 534.

(5) Robaugh, D. A.; Stein, S. E. *Int. J. Chem. Kinet.* **1981**, *13*, 445.

(6) Identified in this paper only to adequately describe the materials used in these experiments. Such identification does not imply recommendation or endorsement by the National Bureau of Standards, nor does it imply that the materials identified are necessarily the best available for the purpose.

(7) Brouwer, L.; Muller-Markgraf, W.; Troe, J. *Ber. Bunsenges. Phys. Chem.* **1983**, *87*, 1031.

(8) (a) Choo, K. Y.; Beadle, P. C.; Piskiewicz, L. W.; Golden, D. M. *Int. J. Chem. Kinet.* **1976**, *8*, 45. (b) Golden, D. M.; Choo, K. Y.; Perona, M. J.; Piskiewicz, L. W. *Ibid.* **1976**, *8*, 381.

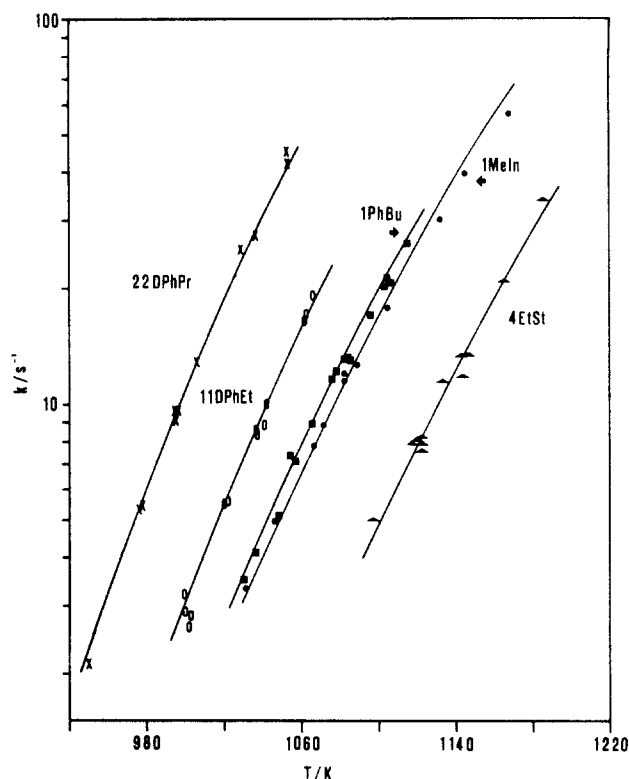
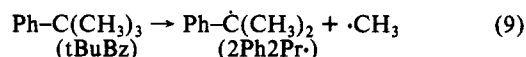
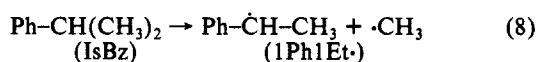
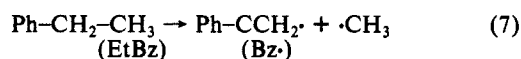


Figure 1. VLPP rate constants. Solid line is RRKM fit to the data.

parent ion peak at 70 eV. The amount of reaction in all cases was reproducible to within $\pm 2\%$ with a signal-to-noise ratio of 50–100 to 1. Conversion of observed mass spectral data to VLPP rate constants was done in the usual way.⁴ VLPP rate constants are plotted in Figure 1.⁹ Rate constants were found to be independent of flow rate; the extent of decomposition varied by only a few percent when flow rates were changed by a factor of up to 34.⁹

Rate Parameters and RRKM Calculations. Measured rate constants are in the fall-off region of unimolecular reactions and were converted to high-pressure rate constants k^∞ by means of RRKM theory.¹⁰ VLPP experiments cannot yield unique sets of Arrhenius parameters; therefore, A factors were estimated and activation energies adjusted to match experimental results.

We chose to estimate A factors for reactions 2–6 by analogy to the decomposition of ethylbenzene (EtBz), isopropylbenzene (IsBz), and *tert*-butylbenzene (tBuBz):



We have previously studied these reactions in the same VLPP apparatus used here⁵ and obtained the following high-pressure rate expressions based on VLPP rate constants, estimated reaction entropies, and the assumption that all reverse recombination rates were equal

$$k_7/\text{s}^{-1} = 10^{15.3} \exp(-36590/T) \quad 1053\text{--}1234 \text{ K} \quad (10)$$

$$k_8/\text{s}^{-1} = 10^{15.8} \exp(-35880/T) \quad 971\text{--}1151 \text{ K} \quad (11)$$

$$k_9/\text{s}^{-1} = 10^{15.9} \exp(-34780/T) \quad 929\text{--}1157 \text{ K} \quad (12)$$

Table II. Comparison of Benzyl C-CH₃ Dissociation Rate Constants, k^∞ , and Corresponding Differences in Activation Energies at $\langle T \rangle$

	$\langle T \rangle$ (K)	$(1/\sigma)k^\infty/(1/\sigma \text{ ref})k^\infty(\text{ref})^a$	$E(\text{ref}) - E$ (kcal mol ⁻¹)
4EtSt	1144	$k_2/k_7 = 1.8$	$E_7 - E_2 = 1.3$
1PhBu	1076	$k_3/k_7 = 11.6$	$E_7 - E_3 = 5.2$
11DPhEt	1041	$k_4/(1/2)k_8 = 5.8$	$E_8 - E_4 = 3.7$
22DPhPr	980	$(1/2)k_5/(1/3)k_9 = 5.8$	$E_9 - E_5 = 3.4$
1MeIn	1082	$k_6/(1/2)k_8 = 4.2$	$E_8 - E_6 = 1.3$

^a σ = reaction path degeneracy.

Table III. Benzyl C-CH₃ Dissociation Rate Constants, k^∞ , at 1070 K

	k^∞ (s ⁻¹)		k^∞ (s ⁻¹)
EtBz	2.9	11DPhEt	56
4EtSt	5.6	1MeIn	62
IsBz	18	tBuBz	63
1PhBu	37	22DPhPr	190

The only correction applied to these A factors in order to estimate A factors for reactions 2–5 was for reaction path degeneracy. Hence we chose A factors of $10^{15.3} \text{ s}^{-1}$ for 4EtSt and 1PhBu with $A_7 = 10^{15.3} \text{ s}^{-1}$ as a reference, $10^{15.5} \text{ s}^{-1}$ for 11DPhEt with $A_8 = 10^{15.8} \text{ s}^{-1}$ as a reference, and $10^{15.7} \text{ s}^{-1}$ for 22DPhPr with $A_9 = 10^{15.9} \text{ s}^{-1}$ as a reference. (As will be discussed later, one additional small correction may be applied to these A factors to account for extra resonance stiffening of internal rotation in reactions 2–5.) For 1MeIn we chose an A factor of $10^{16.0} \text{ s}^{-1}$ with $A_8 = 10^{15.8} \text{ s}^{-1}$ as a reference. Corrections were made for the difference in reaction path degeneracy and for the difference in entropy of activation due to the fact that reaction 6, unlike reaction 8, does not convert an internal rotation to a torsion. A detailed discussion of these A factors is presented later.

RRKM calculations were performed for each molecule with a "vibrational" transition state model^{9,10} constructed to yield the above assumed A factors at the mean reaction temperatures $\langle T \rangle$. Note that it is the Arrhenius parameters that determine the degree of fall-off and not the molecular details of the models used.¹⁰ (We should point out that the temperature dependence of Arrhenius parameters is very dependent on the transition-state model used; therefore as will be discussed later, activation energy differences are first converted to enthalpy differences before extrapolating to 298 K.) By adjusting activation energies to best fit VLPP data (see Figure 1), we obtained the following high-pressure rate expressions:

$$k_2/\text{s}^{-1} = 10^{15.3} \exp(-35930/T) \quad \langle T \rangle = 1144 \text{ K} \quad (13)$$

$$k_3/\text{s}^{-1} = 10^{15.3} \exp(-33970/T) \quad \langle T \rangle = 1076 \text{ K} \quad (14)$$

$$k_4/\text{s}^{-1} = 10^{15.5} \exp(-34020/T) \quad \langle T \rangle = 1041 \text{ K} \quad (15)$$

$$k_5/\text{s}^{-1} = 10^{15.7} \exp(-33060/T) \quad \langle T \rangle = 1000 \text{ K} \quad (16)$$

$$k_6/\text{s}^{-1} = 10^{16.0} \exp(-35230/T) \quad \langle T \rangle = 1082 \text{ K} \quad (17)$$

With use of data from ref 5, values of k^∞ for reactions 2–6 are compared with corresponding rate constants for reactions 7–9 in Table II. Computed activation energy differences (ΔE_a) between each pair of compared homolysis reactions are also provided in Table II. Rate constants have also been extrapolated to a common temperature (1070 K, which is the average temperature of all 8 experiments) in Table III.

ΔBDE and ΔRSE . Activation energies are related to ΔH by eq 18,¹¹ where $E(p)$ is the activation energy for the reverse reaction,

$$\Delta H = E_a - E(p) \quad (18)$$

radical combination, in pressure units. Via eq 18 we directly

(9) See supplementary material.

(10) Robinson, P. J.; Holbrook, K. A. *Unimolecular Reactions*; Wiley: London, 1972.

(11) O'Neal, H. E.; Benson, S. W. "Free Radicals"; Kochi, J. K., Ed.; Wiley: New York, 1973; Vol. 2, 275.

Table IV. Differences in RSE (kcal mol⁻¹)

	SRT		experimental	
	eq 20	eq 21	298 K	(<i>T</i>)
RSE(4VyBz·) - RSE(Bz·)	2.3	1.2	1.6	1.3
RSE(3PhAl·) - RSE(Bz·)	4.3	5.5	[5.4-6.7]	[5.2-6.5] ^a
RSE(DPhMe·) - RSE(1Ph1Et·)	4.2	4.2	4.5	3.7
RSE(DPhEt·) - RSE(2Ph2Pr·)	4.2	4.2	4.0	3.4
RSE(In·) - RSE(1Ph1Et·)			1.2	1.3

^a Error due to uncertainty in the estimated *A* factor. See discussion of *A* factors in the text.

Table V. Thermochemical Data for Molecules of Interest

	<i>S</i> ₂₉₈ ^o (cal mol ⁻¹)	<i>C</i> _p ^o (cal mol ⁻¹)					ref
		300 K	500 K	800 K	1000 K	1200 K	
EtBz	86.15	30.9	49.4	67.2	74.8	80.4	<i>a</i>
IsBz	92.87	36.5	57.9	78.6	87.3	96.1	<i>a</i>
tBuBz	95.93	42.1	67.3	90.9	100.8	106.5	<i>b</i>
4EtSt	101.2	40.9	61.9	82.4	91.3	96.5	<i>c</i>
1PhBu	100.8	39.7	62.0	83.2	92.4	97.8	<i>d</i>
11DPhEt	113.1	49.7	80.2	108.7	120.2	127.0	<i>e</i>
22DPhPr	117.0	55.2	89.6	121.0	133.7	140.8	<i>f</i>
1MeIn	87.2	35.9	56.8	77.4	86.0	91.0	<i>g</i>

^a Reference 17. ^b Reference 18. ^c Estimated by difference from data for *p*-methylstyrene (see footnote *a*). ^d Group additivity¹⁸ estimate. ^e *C*_p^o(11DPhEt) = *C*_p^o(IsBz) + [*C*_p^o(IsBz) - *C*_p^o(isobutane)]. Vir (kcal mol⁻¹): *V*(C-Ph) = 2, *V*(C-CH₃) = 3. Same method was used for entropy. ^f *C*_p^o(22DPhPr) = *C*_p^o(tBuBz) + [*C*_p^o(tBuBz) - *C*_p^o(neopentane)]. Vir (kcal mol⁻¹): *V*(C-Ph) = 2, *V*(C-CH₃) = 3. Same method was used for entropy. ^g Estimated with use of group values of ref 18 and data for indene from ref 19.

equate values of Δ*E*_a (Table II) to differences in reaction enthalpy (Δ*BDE*) at (*T*). This implicitly assumes that activation energies for the reverse of each of reactions 2-6 are equal to the activation energies for the reverse of their corresponding reference reactions (*E*(*p*) is usually set equal to zero, -*RT*, or -(1/2)*RT* for hydrocarbon radical combinations¹).

RSE was defined in eq 1 as the difference between *BDE*(*R*_s-*X*) for a molecule which forms a stabilized radical and *BDE*(*R*_{ns}-*X*) for a reference molecule which forms the structurally related nonstabilized radical. Because both molecules and stabilized radicals in each pair of compared reactions are structural analogues, it follows directly from the definition of RSE that Δ*BDE*(*R*_s-*X*) (which has been shown to be equivalent to Δ*E*_a through eq 18) is equal to the difference in resonance stabilities (Δ*RSE*) of the radicals involved at (*T*) or, more explicitly, Δ*E*_a = Δ*BDE*(*R*_s-*X*) = Δ*RSE*. In each case, values of Δ*E*_a(*E*_a(ref) - *E*_a) are positive, indicating an "extra" amount of RSE in the benzylic radicals of reactions 2-6 relative to those in reactions 7-9. These have been included in Table IV, column 5, and listed as Δ*RSE* at (*T*).

We have also extrapolated Δ*RSE* to 298 K with the aid of eq 19 and heat capacity data provided in Tables V and VI where

$$\Delta(\Delta H^\circ_{T_2}) = \Delta(\Delta H^\circ_{T_1}) + (T_1 - T_2)[\langle \Delta C_p \rangle - \langle \Delta C_p \rangle(\text{ref})] \quad (19)$$

(Δ*C*_p) is the average reaction heat capacity change between *T*₂ and *T*₁. Heat capacities for benzylic radicals and reactant molecules have been estimated by the authors using standard methods.¹² These results are included in Table IV, column 4, and listed as Δ*RSE* at 298 K.

A-Factor Estimates. We now test the validity of our choice of *A* factors and the sensitivity of our results to these estimates.

Our first use of estimated *A* factors was to extract high-pressure rate constants (*k*[∞]) from VLPP rate constants. Small differences in the choice of *A* factor will not substantially affect derived high-pressure rate constants. For example, RRKM calculations were performed for 11DPhEt where the transition-state model was modified to yield *A* factors 10^{0.5} higher and lower than our chosen value of 10^{15.5} s⁻¹. The following rate expressions were obtained, *k*₄/s⁻¹ = 10^{15.0} exp(-32860/*T*) and *k*₄/s⁻¹ = 10^{16.0} exp(-34980/*T*). As expected,¹⁰ both of these rate expressions fit VLPP data as well as *k*₄/s⁻¹ = 10^{15.5} exp(-34020/*T*). At 1041

Table VI. Heat Capacities for Radicals of Interest¹

	<i>C</i> _p ^o (cal mol ⁻¹ K ⁻¹)					ref
	300 K	500 K	800 K	1000 K	1200 K	
Bz·	25.3	40.8	55.2	61.3	64.4	<i>a</i>
1Ph1Et·	30.3	48.3	65.1	72.4	77.7	<i>b</i>
2Ph2Pr·	35.8	56.6	76.1	84.8	93.5	<i>c</i>
4VyBz·	35.4	53.8	70.8	78.1	82.2	<i>d</i>
3PhAl·	34.5	54.0	71.6	78.8	80.1	<i>e</i>
DPhMe·	43.6	71.6	96.5	106.4	114.1	<i>f</i>
DPhEt·	49.2	79.8	107.4	118.6	124.9	<i>g</i>
In·	30.5	47.4	63.6	70.2	74.0	<i>h</i>
CH ₃ ·	8.3	10.1	12.6	14.0	14.9	<i>i</i>

^a Toluene;¹⁷ Vir(Ph-C) = 0 → 12. ^b EtBz;¹⁸ Vir(Ph-C) = 2 → 12, Vir(CH₃-C) = 3 → 2. ^c IsBz;¹⁷ Vir(Ph-C) = 2 → 12, 2(Vir(CH₃-C) = 3 → 2). ^d *p*-Methylstyrene;¹⁷ Vir(Ph-C) = 0 → 13.4, Vir(Ph-Vy) = 2 → 3.4. ^e *β*-Methylstyrene;¹⁷ Vir(Ph-C) = 2 → 7.4, Vir(C-CH₂) = 1 → 17.4. ^f Diphenylmethane;¹⁸ Vir(Ph-C) = 2 → 12, Vir(Ph-C) = 2 → 6. ^g 11DPhEt (Table V); Vir(Ph-C) = 2 → 12, Vir(Ph-C) = 2 → 5, Vir(C-CH₃) = 3 → 2. ^h Indene.¹⁹ ⁱ Reference 12. ^j All heat capacities are estimates of the authors obtained by the difference method.¹² Reference molecules and assumed changes in internal rotational barriers (Vir(kcal mol⁻¹)) are listed in footnotes *a-i*.

Table VII. Predicted RSEs from Structure Resonance Theory in kcal mol⁻¹

radical	CSC(<i>R</i> ·)	CSC(<i>RH</i>)	RSE(eq 20)	RSE(eq 21)
Bz·	5	2	10.0	11.2
4VyBz·	6	2	12.3	12.4
3PhAl·	7	2	14.3	16.7
1Ph1Et·	5	2	10.0	11.2
2Ph2Pr·	5	2	10.0	11.2
DPhMe·	16	4	14.2	15.4
DPhEt·	16	4	14.2	15.4
In·	11	2		

K these rate expressions led to values of *k*[∞] only 13% lower and 15% higher, respectively, than *k*[∞] predicted by rate expression 15. Similar results were found when these calculations were repeated for each of the other molecules studied here.

Our second, and most critical, use of estimated *A* factors was to derive values of Δ*E*_a for each pair of compared homolysis reactions. Uncertainties in relative *A* factors would, therefore, directly affect the Δ*RSE*s obtained here; however, reactions 2-5 and 7-9 are very similar, each involves bond rupture with loss of methyl radical to form a large, resonance-stabilized benzylic radical. From what is presently known about *A* factors for dis-

Table VIII. Comparison of ΔS^\ddagger (cal K⁻¹ mol⁻¹) for 1PhBu and EtBz at 1076 K

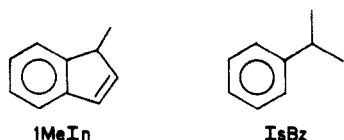
reaction coordinate					
(1) C—C stretch	1000 \rightarrow 0 cm ⁻¹	-1.6	1000 \rightarrow 0 cm ⁻¹	-1.6	0
vibrations					
(2) 2(-CH ₃) bends	1050 \rightarrow 330 cm ⁻¹	4.2	1050 \rightarrow 330 cm ⁻¹	4.2	0
(3) 2(-CH ₂ -) bends	750 \rightarrow 230 cm ⁻¹	4.6	750 \rightarrow 230 cm ⁻¹	4.6	0
internal rotations					
(4) ∞ -CH ₃	V (kcal mol ⁻¹) = 2 \rightarrow 0	0.1	V (kcal mol ⁻¹) = 2 \rightarrow 0	0.1	0
(5) R—Et \rightarrow R—CH ₂	I (amu Å ²) \sim 17 \rightarrow 1.8	-2.2	I (amu Å ²) \sim 17 \rightarrow 1.8	-2.2	0
(6) Barrier Changes	Ph—CHCHCH ₂		Ph—CH ₂		
	V (kcal mol ⁻¹) = 2 \rightarrow 7	-1.0	V (kcal mol ⁻¹) = 2 \rightarrow 12	-1.4	-1.5
	PhCHCH—CH ₂				
	V (kcal mol ⁻¹) = 2 \rightarrow 17	-1.9			

^a $\Delta(\Delta S^{\ddagger} < \text{mo})_{\text{Total}} = -1.5$ cal K⁻¹ mol⁻¹.

sociation of aliphatic molecules, one expects such closely related reactions to have similar A factors. One can test this expectation by using thermochemical kinetic estimates¹³ to compare individual contributions to ΔS^\ddagger .

An example has been provided in Appendix A for the case of 1PhBu and its reference EtBz. Such estimates show that there are only two important contributions to $\Delta(\Delta S^\ddagger)$ for each pair of reactions compared here, namely for reaction path degeneracy, which has already been accounted for in our A factors, and additional resonance stiffening of internal rotation, which we have not accounted for. The latter correction is due to the extra RSEs of the radicals of interest. With use of the procedures of ref 12, estimates of contributions to $\Delta(\Delta S^\ddagger)$ for extra stiffening can be calculated. Estimates for 1PhBu are given in Appendix A. Thus 1PhBu could lose an additional 1.5 cal K⁻¹ mol⁻¹ of entropy due to extra resonance stiffening. This would lower our chosen A factor of $10^{15.3}$ s⁻¹ to $10^{15.0}$ s⁻¹. Using this A factor in RRKM calculations results in an activation energy which is lower by 1.3 kcal mol⁻¹ and to a ΔRSE of 6.5 kcal mol⁻¹ at $\langle T \rangle$ and 6.7 kcal mol⁻¹ at 298 K. These values of ΔRSE have been included in Table IV in brackets along with our first calculated values. When this same line of reasoning is used, estimates for reactions 2, 4, and 5 show that A -factor corrections for resonance stiffening are much smaller. A factors for 11DPhET and 22DPhPr are lowered at most by $10^{0.1}$ s⁻¹ and that for 4EtSt remains unchanged. Thus the assumption that A factors for reactions 2–5 and 7–9 differ only in reaction path degeneracy appears to be reasonable for our present purposes.

Because the structure of 1MeIn is very different from the



structure of its reference molecule IsBz, we felt it appropriate to explicitly account for all contributions to $\Delta(\Delta S^\ddagger)$ in our A -factor estimate. This has been illustrated in Appendix B. The major difference here is that 1MeIn, unlike IsBz, does not convert an internal rotation to a torsion; thus one must add to $\Delta(\Delta S^\ddagger)$ the entropy lost by IsBz in this stiffening. As shown in the Appendix, the total of all contributions to $\Delta(\Delta S^\ddagger)$ amounts to 1 cal K⁻¹ mol⁻¹. Applying this correction to $A_8 = 10^{15.8}$ s⁻¹ yields our estimate for 1MeIn of $10^{16.0}$ s⁻¹.

The major points in this discussion of A factors are (1) K^∞ is not very sensitive to modest changes in assumed A factors, (2) contributions to $\Delta(\Delta S^\ddagger)$ for additional resonance stiffening of internal rotation in reaction 2–5 are not large and can be neglected in A -factor estimates leading to errors in ΔE_a and ΔRSE of ~ 1 kcal mol⁻¹, and (3) an A factor of $10^{16.0}$ s⁻¹ was estimated for 1MeIn from the A factor for IsBz by accounting for all differences in ΔS^\ddagger .

ΔRSEs from Structure Resonance Theory (SRT). We have compared our measured values of ΔRSE with predictions of two forms of SRT. Using SRT for aromatic molecules¹⁴ as a basis, Stein and Golden^{2b} have proposed the following formula for prediction of empirical RSEs for benzylic-type radicals,

$$\text{RSE/kcal mol}^{-1} = A \ln [\text{CSC}(\text{R}\cdot)] - B \ln [\text{CSC}(\text{RH})] \quad (20)$$

where $A = 12.92$, $B = 15.57$,¹⁵ and $\text{CSC}(\text{R}\cdot)$ and $\text{CSC}(\text{RH})$ (CSC for corrected structure count) represent the number of stable Kekulé structures for a radical and its parent hydrocarbon, respectively. These coefficients were derived in the following manner: (1) $B = 27.33$ was taken from Herndon,¹⁴ (2) $A = 22.68$ was then obtained by adjusting eq 20 to reproduce published SCF-MO stabilization energy differences for a series of arylmethyl radicals, and (3) both coefficients were scaled such that eq 20 yields the currently accepted experimental value of $\text{RSE} = 10$ kcal mol⁻¹ for the benzyl radical ($\Delta H_f^\circ_{298\text{K}} = 47.8$ kcal mol⁻¹).¹ Expression 20 has been shown to yield RSE values for the 1-methylnaphthyl and 9-methylantrhylyl radicals in good agreement with recent experimental results.¹ Provided in Table VII are the CSCs for each benzylic radical discussed here along with that for their parent molecules. These have been used in eq 20 to calculate the RSEs in Table VII, column 4.

Herndon has recently presented a different form of SRT for π -radicals.^{2a} He proposed an expression of the form

$$\text{RE/kcal mol}^{-1} = (2/\text{CSC}) \sum H_{ij} \quad (21)$$

where RE is the total resonance energy¹⁶ in the radical and H_{ij} are values of resonance integrals that result from different types of permutations of electron pairs within the radical π -structure. Herndon derived values for six different resonance interactions (H_{ij}). To apply the method one must determine the CSC and number of each type of H_{ij} for a radical and its parent hydrocarbon. RSEs from ref 2a are included in Table VII, column 5, for comparison. As can be seen, predictions of the method of Herndon and that of Stein and Golden are about the same for the radicals considered here.

Predicted values of ΔRSE from SRT are compared to VLPP results in Table IV. Excluding ΔRSE for In \cdot , agreement between the theory and experiment is good. In the case of In \cdot an estimate of ΔRSE has not been provided. Because of its five-membered ring, the CSC for In \cdot is expected to be too large. The problem of over-counting CSCs for radicals containing five-membered rings has been discussed by both Stein and Golden^{2b} and Herndon.^{2a} One solution suggested by Stein and Golden was to simply divide the CSC by two. This leads, in the case of In \cdot , to a predicted ΔRSE of 2 kcal mol⁻¹ compared to the VLPP result of 1.2 kcal mol⁻¹.

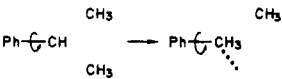
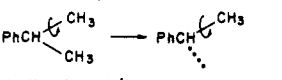
(14) (a) Herndon, W. C.; Ellsey, M. L. *J. Am. Chem. Soc.* **1974**, *96*, 6631. (b) Herndon, W. C. *Ibid.* **1973**, *95*, 2404.

(15) The coefficients reported here are slightly different than those in ref 2b reflecting an adjustment to the presently accepted RSE of 10 kcal mol⁻¹ (see ref 1) for the benzyl radical.

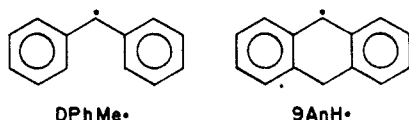
(16) RE is the total π -bonding resonance energy. RSE is defined as the difference between the RE of a radical and the RE of its corresponding parent molecule, e.g., $\text{RSE}(\text{PhCH}_2\cdot) = \text{RE}(\text{PhCH}_2\cdot) - \text{RE}(\text{PhCH}_3)$.

(13) Benson, S. W. *Thermochemical Kinetics*, 2nd ed.; Wiley: New York, 1976.

Table IX. Entropy of Activation (cal K⁻¹ mol⁻¹) Corrections Applied to A_8 (s⁻¹) = 10^{15.8} for IsBz To Estimate an A Factor for 1MeIn

	$\Delta S^\ddagger_{\text{corr}}$
symmetry	$-R \ln 2 = -1.4$
internal rotation	
	2.5
V (kcal mol ⁻¹) = 2 → 12	
I (amu Å ²) ~ 56 → 17	
	
V (kcal mol ⁻¹) = 3.5 → 2.3	
total	-0.2 0.9

It is informative to compare ΔRSE for DPhMe \cdot and its radical analogue 10-hydro-9-anthryl (9AnH \cdot). ΔRSEs of 4.5 kcal mol⁻¹



(present work) and 8 kcal mol⁻¹,¹ respectively, have been determined experimentally. On the other hand, because DPhMe \cdot and 9AnH \cdot have the same formal π -structure their CSCs are the same, so SRT predicts that both radicals should have the same amount of extra resonance stability, 4.2 kcal mol⁻¹. Steric effects in DPhMe \cdot may be the cause of its instability relative to 9AnH \cdot . In DPhMe \cdot one might expect interference between phenyl rings to not allow them to be coplanar, thereby diminishing conjugative stability. Such interference is not expected in 9AnH \cdot which can easily assume a planar conformation. If this explanation is correct, steric effects (σ -bonds) would have to be explicitly taken into account in any general predictive method for RSE. The fact that eq 20 and 21 were scaled to fit the RSE for benzyl radical, which might contain steric energy due to repulsion between methylene and *o*-hydrogen atoms, may explain its accuracy for DPhMe \cdot and related radicals. In any case, development of broader predictive

models requires additional data as well as further theoretical analysis.

Summary

Differences in rates of benzyl C–CH₃ homolysis for reactions 2–6 and 7–9 were used to derive differences in resonance stabilities (RSE) of the benzylic radical products of these reactions. Structure Resonance Theory gave values of RSE in good agreement with our experimental results; however, a significant difference is found between our experimental RSE for DPhMe \cdot and that reported in the literature for the related 10-hydro-9-anthryl radical, despite the fact that SRT predicts that they should have the same values. This difference, along with the result that SRT calculations work for DPhMe \cdot , suggests that steric effects are inherently included in the existing parameters used in SRT calculations. Product mass spectra indicate that reactions 2–6 and 7–9 decompose solely by way of benzyl C–CH₃ homolysis. These results are not consistent with studies of Troe and co-workers of ethylbenzene decomposition where benzyl C–H homolysis was reported to be faster than benzyl C–CH₃ homolysis.

Appendix A

See Table VIII for a comparison of ΔS^\ddagger for 1PhBu and EtBz at 1076 K.

Appendix B

See Table IX for the entropy of activation corrections applied to $A_8/s = 10^{19.8}$ for IsBz to estimate an A factor for 1MeIn.

Registry No. 4-EtSt, 3454-07-7; 1-PhBu, 824-90-8; 22-DPhPr, 778-22-3; Ph₂CHCH₃, 612-00-0; 1-MeIn, 767-59-9; 4-VyBz, 55185-65-4; 3-PhAl, 20671-30-1; MePh₂C, 51314-23-9; Ph₂CH, 4471-17-4; In, 79317-94-5.

Supplementary Material Available: Tables of VLPP rate constants, results of flow rate studies, and RRKM models (8 pages). Ordering information is given on any current masthead page.

(17) Stull, D. R.; Westrum, E. F.; Sinke, G. C. *The Chemical Thermodynamics of Organic Compounds*; Wiley: New York, 1969.

(18) Benson, S. W.; Cruickshank, F. R.; Golden, D. M.; Haugen, G. R.; O'Neal, H. E.; Rogers, A. S.; Shaw, R.; Walsh, R. *Chem. Rev.* **1969**, *69*, 279.

(19) Stein, S. E. *ThermoChim. Acta* **1981**, *44*, 265.

Vaporization of (SN)_x: He I Photoelectron Spectrum and ab Initio Calculations for the S₃N₃ Radical

W. M. Lau,[†] N. P. C. Westwood,^{*‡} and M. H. Palmer[⊥]

Contribution from Guelph-Waterloo Centre for Graduate Work in Chemistry, Department of Chemistry and Biochemistry, University of Guelph, Guelph, Ontario, Canada N1G 2W1, Surface Science Western, Natural Science Centre, University of Western Ontario, London, Ontario, Canada N6A 5B7, and the Department of Chemistry, University of Edinburgh, West Mains Road, Edinburgh, Scotland, United Kingdom EH9 3JJ. Received July 24, 1985

Abstract: The S₃N₃ radical, never previously characterized, is shown to be the major semistable component of the vaporization products of the (SN)_x polymer, as identified by He I photoelectron spectroscopy and in situ quadrupole mass spectrometry. This species can be recondensed to yield the (SN)_x polymer and other colored materials. Revaporization produces S₃N₃ in addition to S₄N₄, S₄N₂, and S₂N₂. Ab initio calculations with better than a double- ζ basis set and including configuration interaction provide evidence for a ²A₂ radical with a planar ring geometry close to D_{3h}. The ground-state cation also has a planar ring geometry with ³A₂' favored over ¹A₁'.

The unusual (SN)_x polymer with its highly anisotropic three-dimensional semimetallic properties, and low temperature superconductivity, has been the subject of considerable interest in

recent years,¹ particularly since it can be incorporated into devices,² and offers prospects for the emerging molecular electronics.³ The conventional production⁴ of this polymer involves preparation and

[†] London.

[‡] Guelph.

[⊥] Edinburgh.

(1) Labes, M. M.; Love, P.; Nichols, L. F. *Chem. Rev.* **1979**, *79*, 1–15.

(2) Scranton, R. A. *J. Appl. Phys.* **1977**, *48*, 3838–3842.

(3) Munn, R. W. *Chem. Br.* **1984**, 518–524.